Icarus 200 (2009) 280–291

Contents lists available at ScienceDirect

Icarus

www.elsevier.com/locate/icarus

Fluidization and multiphase transport of particulate cometary material as an explanation of the smooth terrains and repetitive outbursts on 9P/Tempel 1

Michael J.S. Belton [a,*], Jay Melosh [b]

[a] Belton Space Exploration Initiatives, LLC, 430 S. Randolph Way, Tucson, AZ 85716, USA
[b] Lunar and Planetary Laboratory, University of Arizona, Tucson, AZ 85721-0092, USA

ARTICLE INFO

Article history:
Received 6 August 2008
Revised 15 November 2008
Accepted 20 November 2008
Available online 6 December 2008

Keywords:
Comets, nucleus
Geological processes

ABSTRACT

The Deep Impact mission discovered repetitive outbursts on Comet 9P/Tempel 1 and the presence of several smooth terrains on its surface. We present new measurements of the extent of the smooth terrains, the slopes along their centerlines, and the areas of their likely source regions. Our analysis of these features indicates that they are <700 orbits old and probably the result of an ongoing process. The implications of the recently found locations of the source regions of the repetitive outbursts are also analyzed. We propose that the origins of these phenomena are in the different regimes of fluidization and gas transport in a weakly bound particulate mixture of ice and dust above an assumed amorphous/crystalline H_2O phase change boundary where CO and/or CO_2 gas is released. The depth of this boundary is estimated to lie between 30 and 100 m below the surface. The smooth terrains are visualized as occurring about once every ~70 orbits at random locations of the nucleus where a spurt in CO production occurs over a limited region of the phase change boundary. The weak (tensile strength $\sim 10^2$ Pa) crystalline and dust overburden is locally ruptured and fluidized by the CO gas pressure and is then extruded onto the surface at speeds of ~0.003–0.03 m/s, well below the escape velocity of 1.3 m/s. Once on the surface a base pressure of only 2.5 Pa is required to ensure fluidization of the extruded material and it can remain fluidized for typically ~20 h against diffusive loss of CO. As the material accelerates down the local topography it deflates due to diffusive gas loss. The flow becomes increasingly viscous until it is no longer fluidized at which point it quickly halts forming a terminal scarp. The mean speed of the laminar flow is estimated at 0.3 m/s for an emplacement time of ~3 h. Topographic features on the flow >0.3 m in size should become fully relaxed during the emplacement time explaining the smooth texture seen in the images. In contrast, the repetitive outbursts require a gas-laden reservoir to have formed in the vicinity of the phase change boundary well below their preferred location. We visualize the outbursts to be the result of either spouting or bubble transport to the surface where the release of gas is diurnally modulated by either thermal stresses or H_2O sublimation back pressure. The source region for the i2 smooth terrain is found to coincide with an H_2O-ice rich area and we propose that the process of elutriation, i.e., the separation of different classes of particulates depending on their drag properties, occurs in the fluidized material as it flows up to and through the surface. In this way the material becomes enhanced in H_2O crystals relative to siliceous and carbonaceous particulates.

1. Introduction

At least four ideas have been put forward regarding the origin of the smooth terrains discovered on the surface of 9P/Tempel 1 by the Deep impact mission. Thomas et al. (2007) in their survey of the geology of the surface topography regarded them as the result of "very" fluid flows of material that have been recently emplaced on the surface. Gougen et al. (2008) have pursued this idea and pointed out that if these features are shear flows then, in order for the flow velocity to be lower than the surface escape velocity of 1.3 m/s, the kinematic viscosity of the material involved must be relatively high at $\geqslant 2.5 \times 10^{-3}$ m^2/s. In addition the flow must have had a high Reynolds number ($\sim 10^4$) and was therefore turbulent.

Basilevsky and Keller (2007), believing that eruption of materials from an active interior is improbable, suggested that a geophysical planation process was at work: perhaps a "sublimation driven collapse of relatively steep slopes and the avalanche distribution of the collapsed material within the lows."

Bar-Nun et al. (2008), after dismissing downhill ice creep and sliding as possible explanations, have suggested that the smooth terrains are the result of the deposition of ice grains that were released in a collimated ejection during a massive, but quiescent,

* Corresponding author. Fax: +1 520 795 6220.
E-mail address: mjsbelton@beltonspace.com (M.J.S. Belton).

0019-1035/$ – see front matter
doi:10.1016/j.icarus.2008.11.012

outburst of gas. They envisage that the ice particles are collimated by channels that open up during the outburst and connect the surface to a region in the interior where gas-laden amorphous ice is first annealed and then crystallized in an exothermic phase change.

A quite different kind of explanation was put forward by Belton et al. (2007) who included the smooth terrains in their "talps" hypothesis on the origin of extensive layering seen on the surface. They proposed that they are recently exhumed (by sublimation) primitive layers that were originally laid down during the formation of the nucleus and that were protected from primitive impact and erosional processes by being buried immediately after they were laid down.

However, there is plenty of observational evidence for materials erupting from the interior of Tempel 1. During the days of approach to impact, ten cometary outbursts were observed by the Deep Impact cameras (A'Hearn et al., 2005). These were found to be repetitive and organized into two groups in time (Farnham et al., 2007). They did not repeat with strict periodicity but, nevertheless, had a repetition rate related to the spin period suggesting that two locations on the surface may be involved.

Belton (2008) and Belton et al. (2008), using a stereoscopic method involving observations made by both Deep impact and the Hubble Space telescope (Feldman et al., 2007), subsequently located the source regions of the outbursts on the Thomas et al. (2007) shape model of the nucleus and all appear to originate near the two places where the long principal axis meets the surface, i.e., the regions where the effective surface gravity on the nucleus is lowest.

Most recently Meech et al. (2008) have announced that they are exploring the possibility that the emplacement of the smooth terrains may be similar to that in terrestrial pyroclastic flows but no details are available in their abstract.

In this work we pursue the ideas of Thomas et al. (2007) and Gougen et al. (2008) and seek to show, using the ideas and models for CO production in the interior by Tancredi et al. (1994) and Prialnik and Bar-Nun (1990), that fluidization (Gidaspow, 1994) of the cometary materials above the amorphous–crystalline H_2O boundary and their subsequent transport to the surface in different types of several possible gas/particulate flow regimes is responsible for the smooth terrains and the repetitive outbursts.

In Section 2 we use Deep Impact observations to argue that cometary material down to the amorphous/crystalline H_2O ice boundary has low tensile strength and is highly comminuted. In Section 3 we review what is known about the smooth terrains and offer some new some measurements and interpretations of the Deep Impact images. In Section 4 we review what is known about the Tempel 1 outbursts. In Sections 5, 6 and 7 we consider different aspects of the physical processes that likely occur at the amorphous/crystalline ice boundary and the likely modes in which CO gas and cometary particulates are transported to and flow on the surface. In Section 8 we describe the processes that we propose are most likely to have led to the formation of the smooth terrains and repetitive outbursts.

2. The state and tensile strength of the material above the amorphous–crystalline H_2O-ice boundary

One of the most significant discoveries of the Deep Impact mission, following the artificial impact, was the ease with which the material in the comet's sub-surface was comminuted. A'Hearn et al. (2005) argued that the large volume of "very fine (microscopic) particles" were too many to have been pulverized in the impact itself and that they were either pre-existing as very fine particles or weak aggregates of such particles. Observations of the effect of radiation pressure on the shape of the impact plume observed from Earth indicate that most of the particles have effective diameters between 0.5 and 2.5 μm (Schleicher et al., 2006).

Direct evidence on the typical particle size that exists at the surface of the nucleus is provided by Sunshine et al. (2006) who observed patches of enhanced H_2O ice with the high-resolution infra-red spectrometer and Groussin et al. (2007) who mapped the distribution of thermal radiation over the surface. They found that the H_2O ice was thermally, and therefore physically, decoupled from the dust and that the characteristic size of the water crystals was 30 ± 20 μm.

The composition of the dust component is evidently very diverse and includes silicacous minerals, refractories, and a wide range of organic material (A'Hearn et al., 2005; Harker et al., 2005; Mumma et al., 2005; Lisse et al., 2005). The state of this material is hard to evaluate, but, if we can use the evidence from the Stardust sample return (Brownlee et al., 2006) at another periodic comet, Wild 2, the refractory materials are micron to nanometer sized particles that were weakly aggregated into complex accumulations (Kearsley et al., 2008) and possibly embedded in a "fine-grained, possibly, highly-porous" matrix (Van der Bogert et al., 2008). The porosity of cometary material also follows from the bulk density of $\sim$400 kg/m^3 found for Tempel 1 (Richardson et al., 2007) and similar values found for other cometary nuclei (Weissman et al., 2004).

In their analysis of the ejecta curtain, Richardson et al. (2007) were able to estimate an upper limits to the effective yield strength of the cometary material at the surface in terms of the total ejected mass released. In the case where the total amount of material released was $\sim 10^7$ kg, the yield strength in the immediate sub-surface is "not more than 10^2–10^3 Pa" and could be much less, even strengthless. In cases were the yield strength was assumed to be higher the amount of material released was much less. Remote observations of the mass of H_2O ice released during the impact yield 4.5–9×10^6 kg (Keller et al., 2007) and 1.3×10^7 kg (Schleicher et al., 2006). It seems, therefore, to be an established observational fact that in its upper layers the nucleus material must be a very weak and easy to comminute.

In addition, there may be a theoretical reason why the material at the surface and down to the amorphous/crystalline boundary might be highly comminuted. Gronkowski (2005) has noted that grains of amorphous water ice have slightly different material density to those of the cubic crystalline form and that this "... must cause lots of strains and finally leads to erosion and pulverization of that part of the cometary nucleus that has undergone crystallization." Patashnik et al. (1974), in their original discussion of the role of amorphous ice in comets, also suggested that pulverization to small particulates could accompany the phase transition to crystalline ice. However, it should be noted that Patashnik et al. were thinking in terms of a particularly high density form of amorphous ice that, being formed at high pressure, is probably no longer considered appropriate to the cometary problem. In their laboratory experiments with gas-laden amorphous ice Laufer et al. (2005) do not mention such a process but they do note that in the phase transition the ice can shatter and eject ice crystals. They ascribe these phenomena to the flow of released gas.

A second result from Richardson et al.'s study was an estimate of the effective surface gravity at the impact site of $\sim 3 \times 10^{-4}$ m/s^2, which, given the dimensions of the nucleus (Thomas et al., 2007), leads directly to its mass and a bulk density of $\sim$400 kg/m^3. Following Belton et al. (2007), we find that the hydrostatic stress near the center of the nucleus due to the weight of the overburden is near $\sim 5 \times 10^2$ Pa. Measurements of the compressive strength of cometary material have been made in the laboratory (Bar-Nun and Laufer, 2003). They found a limiting compressive strength of $\sim 2 \times 10^4$ Pa when starting with a loose aggregate of $\sim$200 μm amorphous ice particles. Theoretical estimates have also

been made. For example, Sirono and Greenberg (2000) estimate a compressive strength of $\sim 10^4$ Pa for a porosity of 0.3. Appreciable compression of material in the interior is therefore unlikely.

So far we have only discussed the microstructure of the cometary material. On macro-scales the Deep Impact images show the pervasive presence of layering in exposed scarps. They do not show explicitly how deep into the sub-surface the layering persists, but Belton et al. (2007) have proposed that these layers were laid down in primitive times when the nucleus was formed and persist throughout the entire body of the comet. If this is the case then we can expect that the pulverized, particulate, material above the amorphous/crystalline H_2O ice boundary may still reflect some of the original compositional properties, e.g., dust/ice ratio, of this layering.

In summary, the nucleus material above the amorphous/crystalline H_2O ice boundary is, in all probability, a mixture of complex, possibly highly-porous, aggregates of small particles that embody a wide variety of organic and mineralogical compositions (i.e., cometary dust) and crystalline ice crystals $\sim$30 μm in size that may retain some of the compositional aspects (e.g., dust/ice ratio) of primitive layering. This mixture is expected to be able to substantially resist the low compressive stresses that are expected in the interior, but have very low tensile strength. The tensile strength of nucleus material is probably $\leqslant 10^2$ Pa from the amorphous/crystalline H_2O ice boundary (see below) out to the surface.

3. Properties of the smooth terrains

Three smooth terrains have been found on the part of the surface imaged by the Deep Impact cameras at high spatial resolution ($\sim$25% of the total surface). Evidently they are a relatively common feature, a conjecture that may soon be tested at the Stardust–NExT mission encounter with Tempel 1 in 2011. Thomas et al. (2007) describe the best imaged of these features (i1 and i2) as units that originate on downhill slopes and occupy gravitational lows on the nucleus shape model. They are tongue-like shaped features with "digitate markings suggestive of spreading flow at their distal end" and terminate in a steep scarp. According to Thomas et al., these features, which are completely devoid of craters to scales as fine as 5 m, were emplaced by the flow of "very" fluid material possibly erupted on the surface whose smoothness suggests that they consist of a "very homogeneous, and probably fine-textured material." i1 is described as about 3 km long, 1 km wide and at least 20 m thick. In order to get a better quantitative feeling for these features we have digitized their shapes and laid them down on the shape model in order to compute their areas, dimensions, gravitational slopes, and altitudes referenced to the center of figure. We also infer the volume of i1 and i2 under the assumption of an average thickness that seems typical for Tempel 1. Our results, in Table 1, are consistent with, and supplement, the description given by Thomas et al.

The rough dimensions of what we presume to be the outflow regions of i1 and i2 are also included in Table 1. Both are associated with larger depressed regions. This is most obvious in the case of i2 (Fig. 1) where the source is located just inside the southern boundary of a large circular depression (denoted as g1 by Thomas et al.). It appears to be coincident with a lozenge-shaped, brighter, marking that is also co-incident with one of areas of enhanced H_2O ice found by Sunshine et al. (2006). The source region of i1 is illuminated (barely) by light scattered from the impact plume (Fig. 2) and also appears to be a depression, although we note some uncertainty in this conclusion. The flow emanates from the depressed region in a channel some 180 m wide to the south of an approximately N–S ridge line that forms its eastern boundary. The western boundary is ill-defined in the images and we found

Table 1
Measured and assumed properties of the smooth terrains (flows). Columns 3 and 5 are dimension of the presumed source regions as described in the text. A semicolon indicates considerable uncertainty. In both cases the source of the flow is within the boundary of the source region. i1, i2, and g1 are appellations given in Thomas et al. (2007).

Property of flow or source region	i1 flow	i2 flow	i1 source region	i2 source region (g1)
Length (km)	3.0	3.0	1.6	1.3
Max. width (km)	1.8	1.4	0.7	1.3
Area (m^2)	1.6×10^6	2.4×10^6	7.0×10^5	1.2×10^6
Assumed average thickness or depth (m)	15	15	20	20
Volume (m^3)	2.4×10^7	3.6×10^7	1.4×10^7	2.4×10^7
Coordinates of origin (E. Long, Lat)	248, −76	270, −17	–	–
Estimated dimensions of outflow region (m)	170 × ?	180 × 70	–	–

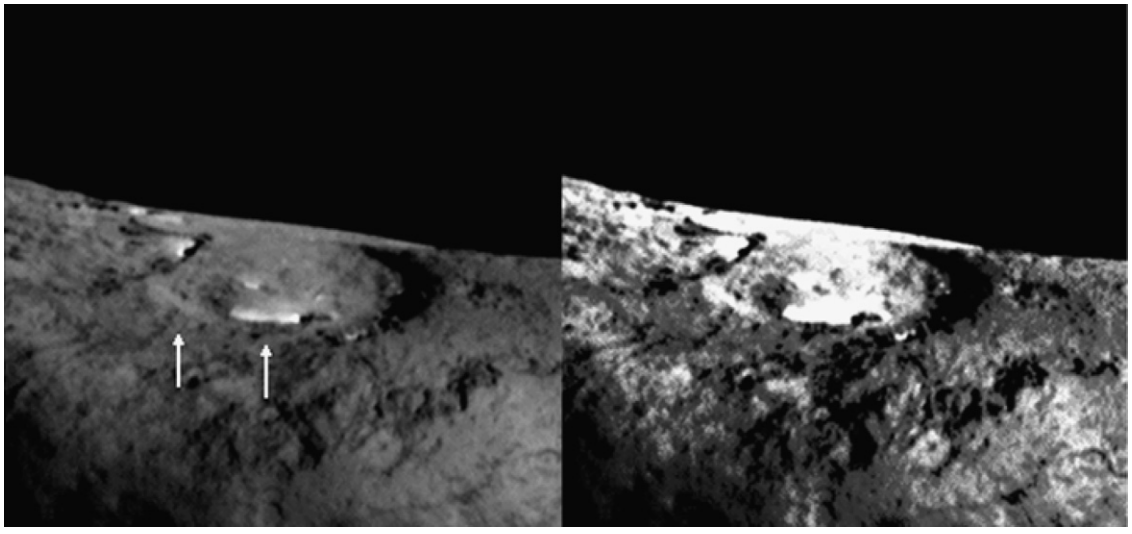

Fig. 1. Image of the source region of the i2 smooth flow (terrain) and the arcuate depression g1 (Thomas et al., 2007). The pixel scale in this image (MV0173728477_9001054_001_RR.FIT) is 9 m/pixel. In the cometocentric frame North is approximately up and West is to the left. The image on the left has been contrast stretched and the bright lozenge-shaped feature (right arrow) inside the southern rim of g1 from which the smooth flow appears to originate is also coincident with one of the regions of enhanced H_2O ice found by Sunshine et al. (2006). The leftmost arrow points to what we suspect is a secondary source. The right image has been filtered with an unsharp mask to bring out the contrast of the flow material.

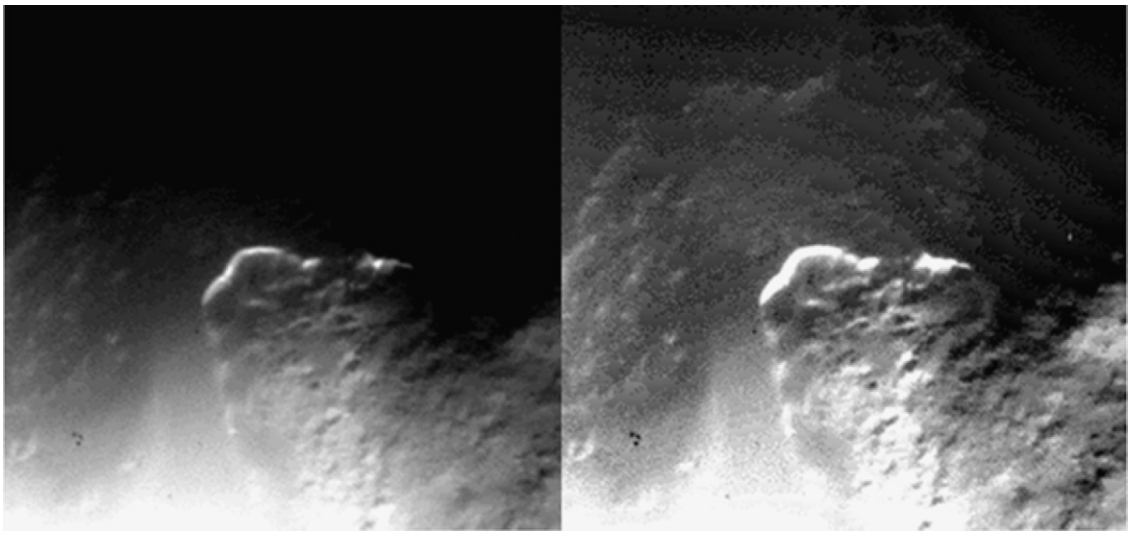

Fig. 2. Source region of the i1 smooth flow (terrain). In this image N is to the right and W is approximately up. The image on the left has been contrast stretched to show the flow emanating to the south of a N–S ridge line. Illumination is provided by light scattered from the impact ejecta plume. The image to the right has been high-pass filtered with an unsharp mask to increase the contrast of the suspected source region for the flow.

its location is hard to determine [Fig. 15 of Thomas et al. (2007) gives an alternative visualization of i1's source region that may help the reader to evaluate the morphology of the surface]. To the extent that we can determine them, estimates of the dimensions of the outflow regions are also given in Table 1. In Fig. 3 we show our results on the run of gravitation height (Thomas, 1993; Thomas et al., 2007) and, for comparison, the radius to the center of figure for the centerline of each flow. The figure show similar dynamic slopes (5–10 deg) to those found by Thomas et al. (2007) near their source and the coverage of i2 is extended to its terminus. The average slope over the entire length of the flows is ∼3 deg. Both flows are now seen to have upturns in gravitational height where they terminate.

In the following discussion of the mechanisms that emplace the flows several questions arise that we anticipate here: (1) was the material in each of the flows emplaced as a single event or were multiple episodes involved? (2) How does the volume of material in each of the flows compare with the volume occupied by the depression that we have associated with their source? (3) What is the age of these flows?

To answer the questions in (1), we have found nothing in the images that suggests other than the main body of each flow was laid down as a single event. While we suppose that it is possible a succession of substantial events might have occurred, where later events have covered up all traces of the earlier ones, there is no evidence of this. However, there are suggestions of later, more superficial, flow activity. For example, in Fig. 4 we note that at least one (and possibly a second) of the digitate markings on i1 seems to overflow the scarp at the terminus of the main flow onto the floor of the adjoining plain. Presumably this must have occurred some time after the emplacement of the original flow. In the case of i2 (Fig. 1), we note a diffuse marking to the west of the main outflow region that connects to the main flow. We suspect that this could be a secondary outflow region but we have found no indications of what the relative timing of the two sources might have been.

Question 2 can be answered more quantitatively given the information in Table 1. The critical unknowns are the thickness of the flows and the depths of the source region depressions. From Thomas et al. we know the thickness of the scarp at the terminus of i1 is 15–20 m. They also find that the eastern boundary of depression g1 (the source region of i1) is up to 40 m in height. In order to proceed we have simply assumed that the average thickness of the flows is 15 m and that the average depth of the source depressions is 20 m. While it is obvious that these assumptions could easily be in error by a factor of a few, this is an unavoidable problem given the information available. Common experience, for example, would suggest that the flows could be much thinner near the source, where the slopes are steeper, than at the terminus where the flows have been halted. Also the topography that has been measured is at the surface of the flows and, therefore, may not properly reflect the topography of the underlying surface. Nevertheless, when these assumptions are adopted we find that the volume in each of the depressions is similar to the volume of

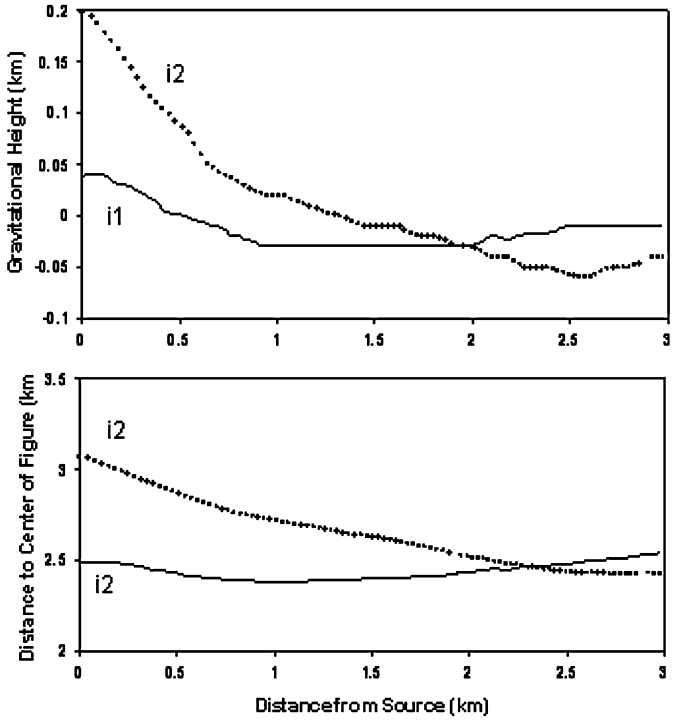

Fig. 3. Visualization of the slope at the centerline of the i1 and i2 smooth terrains. In the upper panel we plot the gravitational height (Thomas, 1993) of the surface of the terrain along the centerline of the flow. In the lower panel we plot the distance to the center of figure. In both cases the flow terminates on an upslope in gravitational height.

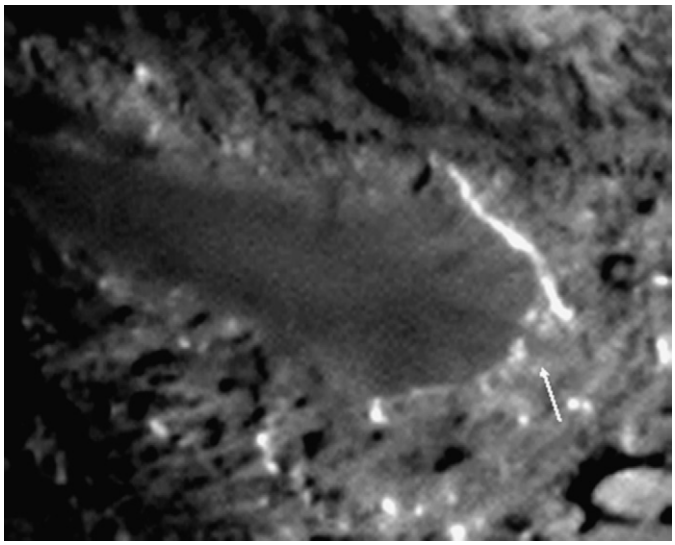

Fig. 4. Evidence of flow activity on the i1 smooth terrain that occurred after the emplacement of the main flow. The image has been contrast stretched and filtered with an unsharp mask. The dark, digitate, markings, first noted by Thomas et al. (2007), are easily seen. The arrow points to material associated with one of these markings that appears to have overflowed the scarp at the terminus of the flow.

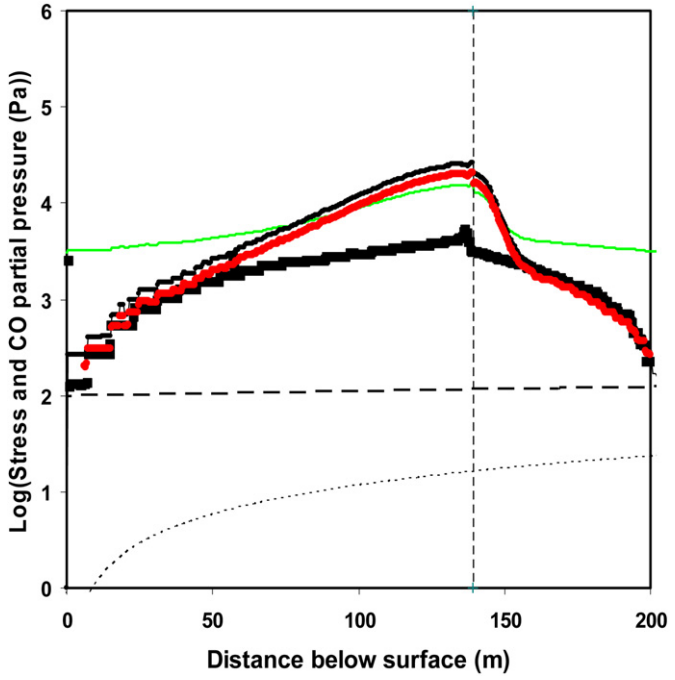

Fig. 5. The partial pressure of CO (black) and radial (red) and tangential stress (green) with depth in the model of Tancredi et al. (1994) in the active (thin line) and quiescent phases (thick line) of their standard model. The radial stress curve for the active phase has been displaced downwards from the active CO pressure line by 0.1 log units in order to make it visible. In actuality these curves plot essentially on top of each other. The stress curves are only shown for the active phase. The vertical dashed line marks the depth (~138 m) of the amorphous/crystalline boundary 87 years into the 500 y integration. The data used to construct this figure was digitized from Figs. 4a and 4b of Tancredi et al.'s paper. The broken nature of these lines at small depths is an artifact of the digitization process. The short-dashed line is an estimate of the maximum overburden stress with depth. The long-dashed line is the expected maximum tensile strength of cometary material. These curves assume a gravitational acceleration of 3×10^{-4} m/s^2 and a density of 400 kg/m^3.

material of the respective flow (cf. Table 1). This, we suggest, provides some support for the idea that the flows and the depressions near their source are physically connected.

To answer question 3 we note the smooth terrains occupy the highest stratigraphic level in the images and have no impact features above 5 m in diameter. The features are either very young (contemporary) or very old (i.e., primitive and quickly covered; Belton et al., 2007), most likely the former. With the average mass loss of ~10^9 kg per orbit (Lisse, 2002; Belton et al., 2007), a mean density of 400 kg/m^3 (Richardson et al., 2007), and a nucleus area of 1.19×10^8 m^2 (Thomas et al., 2007) the average erosion rate is ~0.02 m/orbit. The i2 smooth terrain, which straddles the equator, with a nominal thickness of 15 m should be completely eroded in ~700 orbits or ~5000 y. The smooth terrains, if they are indeed an ice/dust particulate mixture, are possibly as old as, but more likely comparatively young relative to the active lifetime of 3000–25000 y estimated for a typical periodic comet (Duncan et al., 2004). They are therefore most likely the result of an ongoing process. With three smooth terrains seen in the 25% of the surface that was observed by Deep Impact we might expect that there maybe as many as ~12 smooth terrains in various erosional stages in total. If this turns out to be the case, then the above lifetime estimate suggests that a smooth terrain could be formed once every ~70 orbits. While it would be too speculative to suggest a physical connection, we note that this is roughly three times less than the rate at which splittings are observed occur on periodic comets (Chen and Jewitt, 1994).

In summary, new measurements of the i1 and i2 smooth terrains show that they have similar lengths (3 km), areas (~2×10^6 m^2) and, probably, volumes (~3×10^7 m^3). To the extent that they can be located, the linear dimensions (~180×70 m for i2) of the source region from which the flow material originates may also be similar. Both start on relatively steep gravitational slopes and end at an upturn. The terrains were most likely emplaced as a result of a single event, although there is some evidence for subsequent flow activity. The volumes of the flows are also similar to the volumes displaced in depressions associated with their likely source regions, which suggests that there may be a physical connection. The observed rate of sublimation indicates that these features are <700 orbits old and therefore probably the result of an ongoing process.

4. Properties of the repetitive outbursts

The repetitive outbursts on Tempel 1 were discovered in the Deep Impact approach imaging (A'Hearn et al., 2005). They were cataloged by Farnham et al. (2007) who found ten events that fell into two groups when their timing was organized according to the comet's spin period. This suggested that they occurred at two locations on the nucleus. One of the outbursts was also observed from the Hubble Space telescope (Feldman et al., 2007) and Calar Alto Observatory (Lara et al., 2006). This allowed Belton (2008) and Belton et al. (2008) using stereoscopic and statistical techniques to pin-point the two locations on the nucleus shape model. From the images, the locations and timing of the outbursts plus information from other studies of the outburst phenomenon they were able to infer the following properties:

(A) The outbursts occurred both at night and during the day implying that a process in the interior of the nucleus was responsible rather than the effect of direct sunlight.
(B) The locations where coincident with the places on the nucleus that have the lowest surface gravity implying that the process was probably sensitive to the weight of the overburden. This also carries the implication that the overburden material is weak with a tensile strength of no more than 10–10^2 Pa. (This is in agreement with the arguments in Section 2 above.)
(C) The outbursts occurred at times when the surface was cooling and none occurred in the early morning. This suggested to

Belton et al. (2008) that either thermal or gas pressure stresses in the surface boundary layer generated when the surface is cooling may play a role in determining the precise time at which an outburst occurs.

(D) The distribution of brightness in the majority of the outbursts is similar to that of an ejecta curtain. Belton et al. interpreted this to mean that explosive release of gas at the surface and the formation of a crater occurs.

(E) The brightness of the larger outbursts is consistent with the release of $\sim 10^6$ kg of gas and dust.

(F) The signature of the outbursts on the surface of the nucleus is probably a close packed series of depressions ~40 m or greater in diameter.

(G) Because of sparse observational sampling it is possible that an outburst occurs on every rotation cycle—but not in a strictly periodic manner.

(H) The material in the outburst is ejected with a velocity between 60 and 145 m/s (Feldman et al., 2007).

(I) The outbursts are probably driven by CO.

Based on these inferences Belton et al. (2008) suggested a qualitative model of the outburst mechanism in which the release of CO at the amorphous/crystalline H_2O ice boundary periodically inflates and lifts the overburden before releasing the gas at the surface. In the following sections we take a closer look at what happens when CO is released during the amorphous ice phase change and how the gas and cometary particulates might be transported to, and flow on, the surface.

5. The mode, pressure, and timescales of CO release in the interior of 9P/Tempel 1

After H_2O the two most common cometary volatiles are CO_2 and CO. Both of these molecules have been observed in the coma of 9P/Tempel 1: (a) From the Hubble Space Telescope by Feldman et al. (2006), and (b) through the use of the Deep Impact infrared spectrometer by Feaga et al. (2007a, 2007b). Both gases may be involved in cometary activity but the relative extent and domains of each gas is not yet understood. Here, without ruling out CO_2 as a possible contributor, we simply consider CO as the gas responsible for the smooth flows and outbursts. We presume that the detection of CO in the inner coma implies that its origin, or the origin of a substantial fraction, is within the nucleus itself.

The literature documents many investigations that model the source of cometary CO, its evolution, condensation, and transport in the interior. An up-to-date review is given in Prialnik et al. (2004). Broadly there are two kinds of models those with and those without gas-laden amorphous H_2O ice in the interior. We will focus on the former because only that class of model appears to provide an explanation of the outburst phenomenon (Patashnik et al., 1974). Models without amorphous H_2O ice, e.g., that of Benkhoff and Boice (1996), are characterized by low partial pressures, ~0.1 Pa, of CO in the interior (see their Figs. 4 and 5) and we would not expect gas produced in such models to have any bearing on the cause of outbursts and the emplacement of relatively massive flows.

Specifically we consider the model of Tancredi et al. (1994). This model has been taken to task by Bouziani and Fanale (1998) for employing Knudsen diffusion somewhat beyond its range of applicability, but, in our opinion, this flaw is insignificant if the phenomenon of fluidization (Gidaspow, 1994), which we will shortly invoke, is indeed applicable to cometary interiors. The published form of Tancredi et al.'s model is unique in that it explicitly contains the information that we need for understanding the role of fluidization. A close alternative is the model of Prialnik and Bar-Nun (1990). However this model omits the role of the possible condensation of CO below the amorphous/crystalline boundary, which Tancredi et al. find significant. The review by Prialnik et al. (2004) notes other advances in the scope of interior models that have occurred since the work of Tancredi et al. However, these advances are mainly in the direction of understanding the possible response of the assumed pore structure to internal stress in terms of enlargement and crack formation. While we see these studies as important steps in understanding how cometary material might fracture and ultimately become fluidized, we are primarily interested in the internal production of gas pressure and the magnitude of the initial stress fields that can be generated rather than the detailed process by which fluidization might be attained. For this reason we use the well documented Tancredi et al. study as a basis for the work reported here.

In Fig. 5 we show two profiles of CO partial pressure with depth in Tancredi et al.'s Standard Model at times when the crystallization is "quiescent" and when there is an active "spurt" of rapid crystallization. Also shown are curves of radial and tangential stress that we have computed for the active case. The profiles are transcribed from information on number density and temperature in Tancredi et al.'s Figs. 4a and 4b. Superposed on these profiles are curves that indicate the overburden stress due to gravity plus a curve showing the maximum yield (tensile) strength expected (Section 2) for cometary material in the immediate sub-surface. The starting radius of the spherically symmetric nucleus model in Tancredi et al.'s calculations was 3 km and the relevant orbital parameters $q = 1.29$ AU and $Q = 6$ AU are appropriate for a Jupiter family periodic comet. The model nucleus is assumed to be composed of a mixture of dust, amorphous H_2O ice with a 0.1 fraction of trapped CO gas. The many physical parameters that are needed to specify the model can be found in Tancredi et al.'s paper. We note here only that the cometary material in which the transport of CO is followed is assumed to be a *rigid*, porous, matrix. The thermal conductivity of amorphous ice, which ultimately controls the release of CO, was assumed to be a geometric mean of widely disparate estimates by Klinger (1980) and Kouchi et al. (1992). Their standard model was run for 500 years and the profiles in Fig. 5 refer to year 87 of the evolution.

It is clear from Fig. 5 that the stresses caused by the partial pressure of CO at the amorphous–crystalline H_2O ice transition boundary, which has evolved to a depth of ~140 m in the rigid porous matrix after only 12 orbits, are very high relative to the anticipated strength and the overburden weight of cometary material that was discussed in Section 2. That problems would arise from the extraordinarily high partial pressures generated by the release of CO at the boundary was anticipated by Tancredi et al. and, earlier, discussed in more detail by Prialnik and Bar-Nun (1990) and Prialnik et al. (1993). For example, Prialnik and Bar-Nun found pressures of $\sim 5 \times 10^5$ Pa at a depth of only ~12 m in one of their calculations. They suggested that the growing stress on the cometary material above the amorphous ice boundary will in some way expand the pores or rupture the assumed rigid crystalline matrix and thus enhance the escape of gaseous CO to the surface. Prialnik et al. (1993) explored what might happen if the pores in the matrix are allowed to widen under stress or tensile failure occurs. In this way they predicted times of enhanced gas flows (which they associated with cometary jets) and explosions (major outbursts).

Given the low yield strength implied by the Deep Impact observations and the high partial pressures of CO and associated radial and tangential stresses (Fig. 5) produced in the models, the visualization of cometary material above the phase change boundary as a mechanically stable and rigid no longer appears to be appropriate and an alternative physical concept is needed to describe the transport of CO to the surface. Nevertheless, some of the overall evolutionary aspects of Tancredi et al.'s calculations are probably

correct: The ball of gas-laden amorphous H_2O ice as it reaches the vicinity of the Sun is at first very active with unpredictable bursts ("spurts") of crystallization and CO release. This kind of "run-away" phenomenon was also found by Prialnik and Bar-Nun and presumably is due to the strongly exothermic nature of the amorphous to crystalline phase change. As time progresses the amorphous/crystalline phase boundary retreats into the comet's interior leaving an overburden of crystalline ice and dust and run-away spurts of crystallization become less frequent.

To avoid an unbounded secular increase of internal pressure, the mean net production rate of CO at the phase boundary should be roughly equal to the observed CO loss rate which is $4–6 \times 10^{26}$ mol/s (Feldman et al., 2006) or $\sim 4 \times 10^{18}$ mol/s/m^2. Both Tancredi et al. and Prialnik and Bar-Nun find the thickness of the transition layer is $\sim$1 m, which implies a volume production rate near $\sim 4 \times 10^{18}$ mol/s/m^3. If the mixing ratio of CO/H_2O in the amorphous ice is 0.1, a common assumption in this work and a value expected on the basis of laboratory experiments with amorphous ice at temperatures near 25 K (i.e., a temperature near the that at which cometary nuclei are thought to have agglomerated; Bar-Nun et al., 2007), then Schmitt et al.'s (1989) phase change activation law implies a temperature at the phase boundary near $\sim$111 K. (We assume a dust/water ratio of 1 and that half of the CO escapes to the surface. The rest of the CO diffuses into the interior and is condensed there.) If the CO/H_2O ratio is near 0.01 then the temperature is higher, near 117 K. It is interesting that these temperatures fall near the range of 115–120 K where Trancredi et al.'s models show an increase in the rate of crystallization to the point where the phase change becomes self-sustaining. They are, nevertheless, somewhat below the laboratory temperature range of 120–137 K for which Bar-Nun and Laufer (2003) find rapid annealing of the amorphous ice and ultimately its rapid crystallization accompanied by release of trapped gas.

In summary: Using existing models of the propagation of an amorphous/crystalline H_2O phase boundary into primitive cometary material as a guide, we find that the phase boundary is most likely deep within Tempel 1 (depth $\sim$100 m or perhaps more) and that run-away phase transition events (spurts) continue to occur but infrequently. Observations of the production rate of CO indicate that it is being released outwards across the phase change boundary with a flux of $\sim 2 \times 10^{18}$ mol/m^2/s. This implies a temperature range in the vicinity of the phase change boundary of 111–117 K if the mixing ratio of CO_2/H_2O in the amorphous ice is in the range 0.1–0.01. This temperature range is marginally below that at which run-away crystallization would be expected to occur.

6. Fluidization of cometary material in response to the production of CO in the interior and its transport to the surface

We have seen that the paradigm of a rigid, porous, medium that is traditionally used to study the flow of gas through cometary material (Prialnik et al., 2004), can lead to high partial pressures of CO in the interior. This gas pressure produces radial and tangential stresses that could easily overwhelm the tensile or yield strength of the material. In this section we take the view that the assumption of rigidity is unnecessary and that there is plenty of empirical experience from the chemical and power generation industries that shows that the transport of gas in a loose particulate medium may take on properties beyond those of Knudsen and Poiseuille flow that have been considered up to now.

When a gas is forced through a bed of loose particulate material that is constrained in a vertical channel the following phenomena are observed (Gidaspow, 1994, Chapter 5). When the gas input is even across the cross-section of the pipe and the rate of flow is small the gas simply diffuses through the particulate material. At higher rates the pressure head builds up to the point where it can support the full weight of the bed. At this point the particle bed begins to move into an expanded (or inflated) state and diffusive flow no longer applies. Beyond this point bubbles are found to form in the gas/solid multiphase medium and the flow further accelerates the particulates, possibly separating large and small particles (elutriation), and possibly breaking them up at the same time. Further increases in the flow rate leads to larger bubbles that can fill the entire cross-section of the channel and accelerate large "slugs" of particulate material upward, this is sometimes referred to as pneumatic flow. If the gas is injected at a restricted region of the channel's cross-section the phenomenon of "spouting" may occur at sufficiently high flow rates and preferably if the particles are large. In this case the gas forces a channel though the particulate material and escapes at the top of the bed while leading to a circulation of the particulate material in the channel.

The actual behavior of a particle bed is found to depend on the nature of the particles themselves (Gidaspow, 1994, p. 104). If the particles are large (40–500 μm) and dense (1400–4000 kg/m^3), bubbles form easily; if they are small (<40 μm) and light (<140 kg/m^3) the particle bed expands considerably and bubbles form at higher flows; if the particles are cohesive they are more difficult to fluidize and they may cause slugging; If they are large and dense the particle bed has a tendency to spout.

In his book, Gidaspow (1994) develops equations of multiphase transport that can be applied to this problem and investigates the criteria that govern the different types of flow that occur. However, it is not our purpose to build detailed numerical models of the emplacement of the smooth terrains or the occurrence of the outbursts. Here we will restrict our investigation to qualitative models to understand the range of physical possibilities.

7. Variability and stability of gas production at the amorphous/crystalline phase change boundary

Judging by the 25% of the surface imaged by Deep Impact the entire surface of Tempel 1 must be rich in morphological detail. Nevertheless, and with the exception of the sub-solar region where H_2O is clearly subliming at the surface (Feaga et al., 2007a), there are few localities that are obviously active in the images. The two localities where the outbursts occur are clearly at special places (Belton et al., 2008) and represent, at most, only 5% of the total surface area. Extrapolating from the three smooth terrains seen in the Deep Impact images there might be $\sim$12 source regions scattered around the surface. Unlike the case of the repetitive outbursts we know of no association between their locations and the specific geometry of the nucleus. Given the dimensions in Table 1, the source regions of the flows cannot add up to more than $\sim$1% of the surface. There are a few extremely small regions that show weak jet activity (called "surface jets" in Farnham et al., 2007) but again they must represent a small fraction of the total surface area. The main southern jet that was observed for many months up to and through encounter appears to have a diffuse origin over an extended area in the southern hemisphere (Farnham et al., 2007) with no obvious "vents." We have a nucleus that appears to be transporting gas into the coma broadly, if unevenly, over its surface (Feaga et al., 2007a, 2007b) except in special localities, i.e. near the ends of the long axis where the repetitive outbursts occur.

Our interpretation of these facts is that over most of the nucleus surface the sub-surface material is normally mechanically stable and that CO (and/or CO_2) produced in the interior simply diffuses out from their source regions either as a Knudsen or viscous flow. For this to be true, the partial pressures of these gases must always be less than that needed to lift the local overburden. This places a lower limit on the effective diffusivity of the cometary material. In localities where there is an abrupt release

of gas from the interior (outbursts), or where there has been a short-term effusion that has emplaced particulates onto the surface (smooth flows), the mechanical stability of the sub-surface material must have been breached. This indicates to us that either a localized increase in the production rate of gas at depth or a substantial, but localized, change in the diffusivity of the overlying material is responsible. We can think of no convincing cause of the latter and, from this point forward, we will only pursue the idea that short-term increases in the production rate of gas, i.e. spurts, over localized regions of the amorphous/crystalline H_2O ice boundary are the root cause of these phenomena.

The basic reason why spurts of enhanced gas production are seen in the models of Prialnik and Bar-Nun (1990) and Tancredi et al. (1994) lies in the exothermic nature of the phase change (9×10^4 J/kg; Ghormley, 1968) and to heat pulses propagating into the interior as the comet passes through perihelion. For Tempel 1, which we presume to be a "middle aged" comet, the phase boundary is, according to Tancredi et al., already deep in the nucleus (~100 m or greater). We do not expect heat pulses to be either substantial, or localized, by the time they have propagated down to the phase boundary. Nevertheless, the irregular shape of the nucleus and possible spatial variability of the conductive properties of the overburden should lead to variations of temperature and hence CO production over the phase change boundary surface. The crystallization process will continue to proceed in spurts as described by Tancredi et al. (1994) and Prialnik and Bar-Nun, but at different times with different rates at different locations.

It is also possible that the properties of the gas-laden amorphous ice may have its own intrinsic dependence on locality reflecting how the nucleus was put together in the first place. For example, the downward propagating phase change boundary may run into a local reduction in dust/ice ratio that could lead to uneven propagation of the boundary and locally enhanced CO production.

Tancredi et al. (1994) report the results of numerical experiments in which they compare the results of their standard model to results of "variant" models with different dust/ice ratio, porosity, and amorphous ice conductivity. For example, a doubling of the dust/ice ratio slows down the propagation of the phase boundary into the interior and cuts down the average CO production rate. The spurts of crystallization, nevertheless, are still found to occur with essentially the same regularity. Increases in porosity and ice conductivity are found to dampen the tendency for spurts to occur.

In summary, we anticipate that the production of CO at the phase change boundary is variable over the surface of the boundary and consequently the outward diffusion of CO (and possibly CO_2) will be uneven over the surface of the nucleus. When runaway spurts of crystallization occur, we expect that they will be spatially restricted and occur at random locations at unpredictable times.

8. The origin of the smooth terrains and repetitive outbursts on 9P/Tempel 1

The conclusions of the preceding sections provide a qualitative basis for understanding the possible origins of the smooth terrains and repetitive outbursts.

8.1. Smooth terrains

We hypothesize that these are formed at random times and at random placements on the nucleus above locations where the amorphous/crystalline H_2O ice phase change boundary is undergoing a run-away spurt of crystallization of exceptional magnitude and therefore CO production. The resulting increase in gas pressure inflates and ultimately fluidizes the overburden, while the implied radial and tangential stresses overcome the low tensile strength of the cometary material initiating an interior flow towards the surface. This is superposed on a general background production of CO that is both ongoing and uneven over the entire phase change boundary surface. This uneven background diffusive flow may be responsible for the primary jet activity that is characteristic of comets including Tempel 1. While the physical processes involved in initiating enhanced "spurts" are not understood, they could, perhaps, be associated with a localized decrease in (dust/amorphous ice) ratio of primitive origin in the cometary material.

Table 2
Depth of the amorphous/crystalline H_2O ice phase change boundary, D_{fluid} (meters), estimated for different values of the tensile strength and mean free path in the crystalline layer above the boundary. The most likely values of these quantities are near 10^2 Pa and 15 μm for which $D_{fluid} \sim 100$ m.

Tensile strength (Pa), T_e	Mean free path, d_p (μm)		
	10	30	50
10	5	19	36
10^2	54	186	360
10^3	545	1860	3600

The area of the phase change boundary involved in forming a smooth terrain can be deduced by requiring a causal relationship between the depressions surrounding the source regions and the material in the flows themselves. The area involved should be roughly equal to the area of the depressions, $\sim 10^6$ m^2. The typical volume of material to be emplaced on the surface, $\sim 3 \times 10^7$ m^3, places a conservative lower limit to the depth of the phase change boundary at 30 m (i.e., it must be at least 30 m below the surface). The speed of the emplacement flow for i2, which we take as typical, can be estimated as follows: The area at the source of i2 is $\sim 1.3 \times 10^4$ m^2 (Table 1) and the volume of the flow is 3.6×10^7 m^3. According to Tancredi et al. (1994), the timescale of a CO spurt is ~1–10 days. This estimate leads to an outflow speed ~0.03–0.003 m/s, well below the escape velocity of 1.3 m/s, i.e., sub-surface material is slowly extruded onto the surface as a result of fluidization and expansion. On reaching the surface (Fig. 6) the fluidized cometary material begins to release its CO (or CO_2) gas by diffusion to the coma and how it does this will determine the observable coma activity that will ensue. For example, depending on the initial gas pressure in the fluidized material, a major outburst could accompany its initial appearance at the surface. We would expect that such explosive activity would quickly cease as the gas pressure in the material falls and as it continues to be extruded onto the surface. Once on the surface the essentially frictionless material will feel the local slope and flow downhill at speeds governed by its changing kinematic viscosity (see below) until, when finally out of gas, the flow is halted. This speed must be less than the escape velocity of 1.3 m/s as pointed out by Gougen et al. (2008). H_2O-ice crystals would be a major component of the extruded material and at the surface of the flow we anticipate that they would sublime rapidly down to the thermal skin depth (~ few cm; Sunshine et al., 2007) in a few orbital periods ($\sim 2 \times 10^6$ s). Within the bulk of the flow the H_2O component is unlikely to experience any solar heating in the 10^4 s (see below) that it takes to emplace the flow. Sublimation processes are therefore unlikely to effect its dynamics.

With the phase change boundary at depth D, incipient fluidization of the crystalline/dust layer overburden is reached when the CO pressure gradient applies radial and tangential stresses (Fig. 5) that can overcome the yield (tensile) strength plus the hydrostatic stress exerted by the gas and particulates above, i.e., $\sim 10^2 + g\rho_B D$ Pa where g is the local gravity and ρ_B is the bulk density. For example, if the phase boundary is at a depth of 300 m, $g = 2.8 \times 10^{-4}$ m/s^2 and $\rho_B = 400$ kg/m^3, the critical pressure to reach incipient fluidization of the crystalline particulate layer

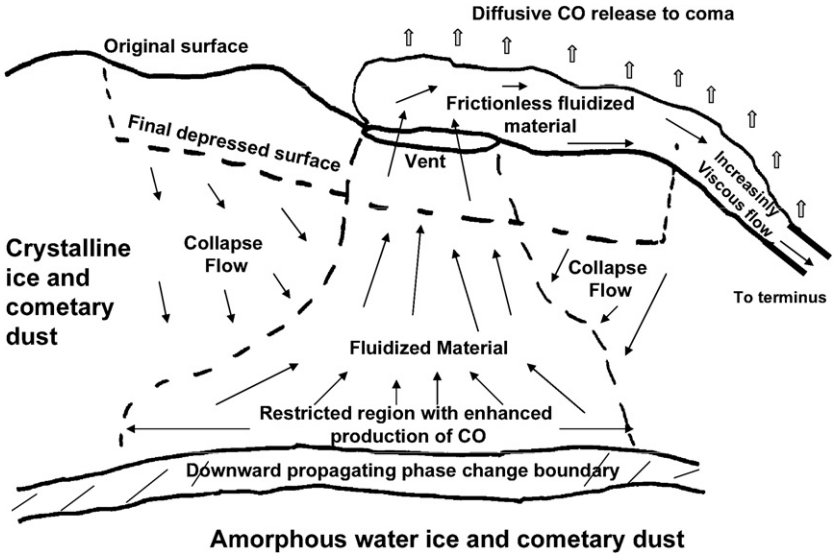

Fig. 6. A schematic view of how a region of smooth terrain might be formed. Over a limited region of the amorphous H_2O ice/crystalline ice phase change boundary there is an enhanced region of CO production near ~100 m depth, i.e., a localized spurt in CO production. The pressure gradient exerts stresses that overcome the tensile strength of the crystalline ice/dust mixture and support it against gravity. The crystalline ice/dust layer is in a state of incipient fluidization. Once the tensile strength has been overcome, the CO production expands the fluidized region and, if the flow rate is high enough, overwhelms the settling speed of the particulates and extrudes the fluidized material onto the surface at low velocity (~0.03–0.003 m/s). The extruded, gas-laden, material is, at least initially, fluidized and essentially frictionless. It accelerates downhill attaining an average speed of ~0.3 m/s while continually losing its gas content. As the material deflates, friction increases rapidly and the flow quickly terminates forming a scarp at its terminus. As the fluidized material leaves the subsurface, surrounding material that was not fluidized, collapses inward to form a depression around the source region.

above would be ~130 Pa. As we have already noted the models of Tancredi et al. and Prialnik and Bar-Nun can easily generate such pressures. Thus the phase change mechanism, through the medium of CO, produces a secular increase of stress at depth that soon overcomes the yield strength of the material.

An upper limit to the depth, D_{fluid}, of the phase boundary can be estimated, in terms of observed quantities by combining the above fluidization criterion with Fick's law of diffusion. With K as the gas diffusivity in the overburden, J_{CO} the flow of CO, T the temperature, T_e the tensile strength, g the local gravity, k the Boltzmann's constant, and ρ_B the bulk density we find in the isothermal case:

$$D_{\text{fluid}} = T_e/(J_{CO}kT/K - g\rho_B).$$

This expression relates the pressure gradient required to maintain the diffusive flow of CO to the weight of the fluidized overburden. We have the following "observed" quantities: $J_{CO} = 4 \times 10^{14}$ mol/cm^2/s (Feldman et al., 2006; Thomas et al., 2007), $g = 2.8 \times 10^{-4}$ m/s^2 (Thomas et al., 2007), $\rho_B = 400$ kg/m^3 (Richardson et al., 2007). For the temperature we take 111 K as computed in Section 5 based on the amount of amorphous ice that needs to be crystallized to produce the observed flow of CO when the fraction of CO to H_2O molecules is 0.1. If, in reality, this fraction is found to be lower, then the temperature could be higher. For the diffusivity, K, the models of Tancredi et al. (1994) and Prialnik and Bar-Nun use formulations for Knudsen and Poiseuille flow suitable for a porous medium with capillaries. Here, since we are considering a loosely packed, low strength, particulate medium we use the simple form from kinetic theory: mean free path x average velocity. We write $K \sim d_p\sqrt{(3kT/\mu)}$ where we associate d_p with the mean particle radius (~15 μm; Sunshine et al., 2006) and μ is the molecular weight of CO. In Table 2 we give D_{fluid} for a range of T_e and d_p that are appropriate for this problem. Our evaluation of the entries in Table 2 is that the phase boundary on 9P/Tempel 1 is probably at a depth ~90 m below the surface. This suggests that the current depth of the phase change boundary on Tempel 1 may lie between $30 < D < 100$ m. These limits ensure that there is enough material to transport to the surface to create the smooth terrains when a spurt of CO production occurs and that the crystalline layer can remain packed for most of the time.

8.2. Dynamics of the smooth outflows

If the smooth outflows observed on the surface of Tempel 1 are indeed the result of gas-fluidized eruptions, several deductions can be made about their dynamics. The outflows, described by Thomas et al. (2007), are smooth-surfaced, uncratered plateaus about 3 km long whose breadth increases markedly near its downslope terminus, resulting in a trumpet-shaped outline. The terminus of the principal outflows is a scarp is 15–20 m high, which we take to indicate the average thickness of the deposits. The flows typically descend a total gravitational elevation of about 150 m for an average surface slope of 3°. The best imaged flow is longitudinally striated, very similar in overall appearance to similar striations on the surface of catastrophic landslides on the Earth (Shreve, 1966) and Mars (McEwen, 1989) that also spread out near their termini.

On Earth, the maximum speed of such landslides is accurately estimated by neglecting friction and equating the gravitational energy of descent to their kinetic energy (Melosh, 1986). Recognizing that this may be an underestimate for the Tempel 1 flow because the mass of fluidized material may have been ejected well above the surface in a strong gas outburst, this method gives a mean velocity of about 0.3 m/s. This implies an emplacement time of 10^4 s, or about 3 h. Supposing that the flow was fluidized by entrained gas, we can show that the time scale for gas expulsion was at least this long.

The flow of gas through a porous material is described by the Darcy equation. Although the application of this equation to a gas under terrestrial conditions yields a nonlinear equation for the pressure (Carman, 1956), the pressure of CO at the base of the 20 m thick flow on Tempel 1 was only about 2.5 Pa to maintain the fluidized state, which at 300 K (the possible surface temperature) implies a mean free path of about 1 cm, far longer than the likely spacing between the grains making up the flow. Under these conditions the flow is in the Knudsen regime and the pressure obeys a diffusion equation with diffusivity D given approximately by:

$$D \sim a\bar{v},$$

where a is the grain size and $\bar{v}$ is the mean molecular velocity (Carman, 1956). For CO at 300 K this is about 500 m/s, so for a grain size of 10 μm, D is about 5×10^{-3} m^2/s. Applying this diffusivity to the pressure equation, the time scale for the gas to leak out of a landslide of thickness h is thus

$$t_{\text{leakage}} = h^2/D.$$

The leakage time scale for a 20 m thick flow is thus about 8×10^4 s, or about 20 h, comfortably longer than the estimated duration of the flow phase.

The viscosity of a dense, flowing granular material is very difficult to estimate. For the flow to occur at all, the grains must be at least expanded to the extent that the particle bed is dilatent. In the case of a very dilute suspension the theory of granular temperature (Gidaspow, 1994) can be applied to 10 μm grains to give a viscosity estimate of about 3×10^{-4} Pa s. This is certainly low enough to permit the nearly frictionless emplacement of the flow: For a flow controlled by viscosity alone, the mean flow velocity is

$$\bar{v} = \frac{\rho g h^2 \sin\theta}{\eta},$$

where ρ is the density of the flow (400 kg/m^3 for Tempel 1), g the acceleration of gravity (3×10^{-4} m/s^2) and η is the dynamic viscosity. If the viscosity of a dilute suspension controlled the flow, it could have moved at 8 km/s before friction slowed it down! Clearly, such a viscosity did not impede its flow. This suggests that the flow was not fully fluidized and that strong grain–grain interactions typical of a dense flow were occurring.

The physical state of the Tempel 1 flow is rather reminiscent of the flow of terrestrial water-saturated debris flows, in which the pressure is also described by a diffusion equation (this differs from terrestrial pyroclastic flows, in which the nonlinear pressure equation regulates the gas flow). Although a great deal of work has been done on such flows, it is still not possible to accurately estimate their viscosity from first principles (Iverson et al., 1997). Grain flow mechanisms also suggest a very low viscosity in the case of such flows, which is not realized in practice: The actual process of fluidization seems to be related to strong pore pressure fluctuations in the mass of the material (Iverson and LaHusen, 1989). A crude estimate of the viscosity is given by $\eta \sim \rho h \bar{v}$, mainly on dimensional grounds, presuming that the pressure fluctuations are due to motion over an irregular bed. Evaluating this expression for the Tempel 1 landslide gives a viscosity of 2.4×10^3 Pa s, which is actually somewhat too high for the estimated velocity: It can be no larger than about 100 Pa s, or else the viscous drag would decrease the mean velocity below our estimate of 0.3 m/s. Nevertheless, this is roughly the right range, suggesting that the flow was indeed fluidized, but as a very dense flow, just above the threshold for fluidization. This accords well with the observation that the flow apparently came to an abrupt stop, ending in a steep scarp. Our interpretation of the scarp is thus that the flow stopped when enough gas escaped to deflate the flow below the dilatancy limit, at which point the grains then locked up and sliding friction became dominant. Under such conditions the flow could not have moved more than a few times its own thickness after deflation, and the scarp would stand at the angle of repose, as it is presently observed to do.

Another way to estimate the flow velocity is to note that the regular longitudinal striations indicate that the flow was laminar, not turbulent. Such laminar flow is, surprisingly, also observed in catastrophic terrestrial landslides. Even though these landslides achieve velocities in excess of 50 m/s, initial stratigraphy in the source area is generally preserved all the way to the terminus of the slide lobe, demonstrating overall laminar flow (Melosh, 1986). Thus, using the knowledge that the Reynolds number Re of the flow was less than about 100, and recalling that $\text{Re} = \rho \bar{v} h/\eta$, we require a viscosity larger than 25 Pa s, again suggesting a dense, partly interlocking, fluidized flow, and consistent with our previous estimates for such a flow.

The low viscosity, between 25 and 100 Pa s, estimated by these methods is also in good agreement with the extremely smooth topography of this terrain (smooth on the scale of the image resolution, a few meters). The relaxation time τ_R for topographic features on a viscous substratum is a function of the size of the breadth feature, so that for a given viscosity and relaxation time we can compute the maximum wavelength feature that can persist (this is identical to the computation of the erasure time of impact craters on a viscous substrate). Thus, surface topography with a wavelength greater than L, where $L = \eta/(0.3\rho g \tau_R)$, is erased over the relaxation time (Melosh, 1989). Inserting a viscosity of at most 100 Pa s and a relaxation time of 10^4 s, we find that surface features broader than about 0.3 m are erased from the flow. Only features maintained dynamically by the flow, such as the striations, can persist at longer wavelengths. This, then, explains the very smooth character of the outflow deposits and places yet another constraint on the viscosity of the flow.

In summary, the smooth terrains on Tempel 1 are consistent with being emplaced as dense gas-fluidized flows that erupted from beneath the surface, perhaps associated with a random outburst event, and flowed away from their sources down the local gravitational gradient (Fig. 6). Due to their high density and thus relatively high viscosity, these flows traveled in a laminar regime and halted abruptly as the fluidizing gas escaped, leaving a steep terminal scarp. Nevertheless, their viscosity was not high enough to seriously impede their flow, which was nearly frictionless during most of their travel. The time scale for emplacement was a few hours.

8.3. Repetitive outbursts

Because these outbursts occur with some regularity they cannot originate as a result of random spurts of crystallization as was the case discussed above for the smooth terrains. We propose to model the repetitive outbursts based on the either the phenomenon of "bubbling" or "spouting" over a sub-surface reservoir of CO. The source of the gas is nevertheless still assumed to be the result of the annealing and crystallization of gas-laden amorphous ice but, to provide a basis for a regular process we invoke the idea of a reservoir in which the released CO can collect and then be released periodically. The reservoir does not need to be a complete void in the nucleus structure but should have high porosity relative to its surroundings. Some of the gas could even be stored below the phase change boundary bounded from below by CO ice. There is a second argument for the existence of such a reservoir to explain this phenomenon and this concerns the quantity of gas released. With approximately $\sim 10^6$ kg of gas and solid particulates in the larger outbursts at an occurrence rate of every 1.7 days, the average gas flow rate could be as high as $\sim 8 \times 10^{25}$ mol/s if the gas and solids are equally represented. This is a substantial fraction, ~16%, of the observed total CO production rate for the entire nucleus of $4–6 \times 10^{26}$ mol/s. Evidently the gas must be collected from a wide area of the phase change boundary, $\sim 2 \times 10^7$ m^2 (equivalent radius = 2.5 km), i.e., and collected into a sub-surface reservoir before being released in an outburst. This "collection area" is, in itself, a rough measure of the lateral size of the reservoir.

For *spouting*, the source of gas flowing through the cometary sub-surface should be localized so that it can fluidize a narrow channel and ultimately escape at the surface. The upper region of the reservoir should be either "conically" shaped or extend in a narrow channel into the upper layers. The observations show that

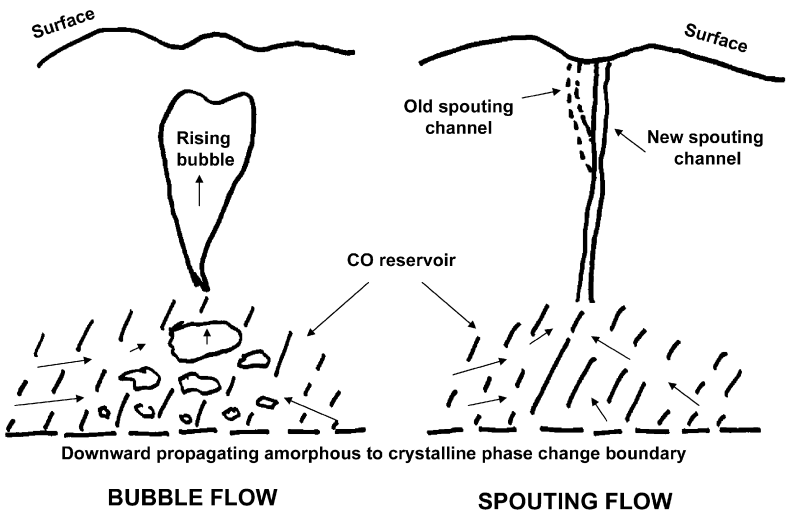

Fig. 7. Two possible mechanisms for the origin of repetitive outbursts on Comet Tempel 1. The left panel represents the formation of a large bubble that rises to the surface buoyantly. It reaches the surface only when the back pressure of sublimating H_2O falls in the afternoon and night time. On the right the gas is released only when the geometry of the upper regions of the CO reservoir is suitable for the formation of a spouting channel in the comet sub-surface. In both panels the nucleus of Tempel 1 is depicted in schematic cross-section and shows the phase change boundary and the formation of a gas reservoir below the end of the long axis. The reservoir may straddle the phase change boundary and are bounded at lower regions by CO ice.

the outburst, i.e., the opening of the channel, is evidently moderated by thermal processes at the surface itself (see Section 4). Since the outbursts tend to occur when the surface is cooling, we speculate that the increasing back pressure exerted by the sublimation of water during the morning might prevent the narrow fluidization channel from reaching the surface at that time. This pressure is relieved in the late afternoon and evening as the H_2O sublimation flux declines presumably allowing the outburst to occur. While such a mechanism provides a simple explanation of why the frequency of outbursts is tied to the diurnal spin rate it may have serious problems: The vapor pressure of H_2O over ice at its free sublimation temperature of ~200 K at 1.5 AU is only 0.15 Pa — insignificant for this problem. However, according to Groussin et al. (2007) temperatures between 272 and 336 K are observed occur over much of the sunlit hemisphere of Tempel 1. If there is good thermal contact between the dust and ice and it is these temperature values that determine the sublimation pressure of H_2O in the very upper layers of the comet then vapor partial pressures of 6×10^2 Pa and greater are a possibility. At this pressure level the generation of water vapor might have the desired effect of modulating the occurrence of the outbursts. Only detailed calculations can settle this issue.

For *bubble* flow, there are no particular requirements on the geometry of the upper regions of the reservoir. We envision that bubbles form in the weakened particulate medium that eventually coalesce into a single large construct that buoyantly rises to the surface. In the vicinity of the surface we invoke the same triggering mechanism described above. As the back pressure falls the bubble reaches the surface and simply bursts releasing the gas instantaneously. We can make a rough estimate of the dimensions of the bubble while en route to the surface and, as will be seen, this leads to a problem for the concept. To overcome the yield strength of the cometary material a gas pressure of $\sim 10^2$ Pa is required in the bubble. With an ambient temperature near 130 K (Tancredi et al., 1994), the bubble must carry $\sim 5 \times 10^5$ kg of CO to satisfy the observations. With these parameters the diameter of a spherical bubble would be ~0.7 km! While rising to the surface the bubble would be far from spherical and would be expected to present a far smaller cross-section in the direction of motion and be considerably elongated. The large size of the bubble may be the nemesis of this concept for in order for the bubble to be free of the reservoir, the reservoir and its associated phase change boundary would have to be at a considerable depth, i.e. >0.7 km or a quarter of the effective radius of the nucleus.

Both of the above scenarios depend on the formation of adequate reservoirs for the gas at the two ends of the long axis of the nucleus (Fig. 7). Why this should happen is not understood.

9. Discussion

The ideas expressed above lead to a number of predictions that could be tested by the NExT mission that will encounter Tempel 1 in 2011, the EPOXI mission to Comet Hartley 2 half a year earlier, and by ESA's Rosetta mission in 2014. At Tempel 1 smooth flows would be expected to be seen on the parts of the surface not previously imaged by Deep Impact. The repetitive outbursts may still be occurring on Tempel 1 and copious amounts of CO could be associated with them. Craters associated with source region of the outbursts should be seen in closely packed arrays. Arcuate or irregular depressions should surround the source regions of all the smooth flows and there may be enhanced CO emission associated with the source regions. Similarly, the Rosetta mission has many experiments relevant to the ideas and phenomena discussed in this paper. We note in particular the CONSERT experiment which will probe the interior structure of the nucleus of the target comet by microwave transmission.

Finally we would like to bring to the reader's attention the phenomenon of elutriation (described briefly in Section 6) which can occur in fluidized granular flows. In a given size range lighter particles tend to be separated from heavier ones and move upward faster (actually falling more slowly relative to the gas flow). It has occurred to us that this phenomenon could possibly explain why the source region of the i2 flow has a higher albedo than the surrounding region and why the area has enhanced water content. If this is the case then the water crystals, if they are indeed physically separate from the dust (cf. Groussin et al., 2007), should typically have a Stokes settling velocity in CO that is greater than that of the dust particles.

Acknowledgments

We thank Peter Thomas for supplementing our PDS-Small Body Node Shape model of 9P/Tempel 1 with surface gravity and gravitational height information. This research was performed with the

University of Maryland under contract NNM07AA99C, and Cornell University under agreement 51326-8361.

References

A'Hearn, M.F., and 28 colleagues, 2005. Deep Impact: Excavating Comet Tempel 1. Science 310, 258–264.

Bar-Nun, A., Laufer, D., 2003. First experimental studies of large samples of gas-laden amorphous cometary ices. Icarus 161, 157–163.

Bar-Nun, A., Notesco, G., Owen, T., 2007. Trapping of N_2, CO, and Ar in amorphous ice—Application to comets. Icarus 190, 655–659.

Bar-Nun, A., Pálsson, F., Björnsson, H., 2008. Formation of smooth terrain on Comet Tempel 1. Icarus 197, 164–168.

Basilevsky, A.T., Keller, H.U., 2007. Craters, smooth terrains, flows, and layering on the comet nuclei. Solar Syst. Res. 41, 109–117.

Belton, M.J.S., 2008. The source region of the 2005 June 14 and other mini-outbursts on Comet 9P/Tempel 1. The case for active cryo-volcanism. Lunar Planet. Sci. 39. Abstract #1086.

Belton, M.J.S., Thomas, P., Veverka, J., Schultz, P., A'Hearn, M.F., Feaga, L., Farnham, T., Groussin, O., Li, J.-Y., Lisse, C., McFadden, L., Sunshine, J., Meech, K.J., Delamere, W.A., Kissel, J., 2007. The internal structure of Jupiter family cometary nuclei from Deep Impact observations: The "talps" or "layered" pile model. Icarus 187, 332–344.

Belton, M.J.S., Feldman, P., A'Hearn, M.F., Carcich, B., 2008. Cometary cryo-volcanism: Source regions and a model for the UT 2005 June 14 and other mini-outbursts on Comet 9P/Tempel 1. Icarus 198, 189–207.

Benkhoff, J., Boice, D.C., 1996. Modeling the thermal properties and the gas flux from a porous, ice-dust body in the orbit of P/Wirtanen. Planet. Space Sci. 44, 665–673.

Bouziani, N., Fanale, F.P., 1998. Physical chemistry of a heterogeneous medium: Transport processes in comet nuclei. Astrophys. J. 499, 463–474.

Brownlee, D.E., and 183 colleagues, 2006. Comet 81P/Wild 2 under a microscope. Science 314, 1711–1716.

Carman, P.C., 1956. Flow of Gases through Porous Media. Academic, New York.

Chen, J., Jewitt, D., 1994. On the rate at which comets split. Icarus 108, 265–271.

Duncan, M., Levinson, H., Dones, L., 2004. Dynamical evolution of ecliptic comets. In: Festou, M., Keller, H.U., Weaver, H.A. (Eds.), Comets II. University of Arizona Press, Tucson, pp. 193–204.

Farnham, T.L., Wellnitz, D.D., Hampton, D.L., Li, J.-Y., Sunshine, J., Groussin, O., McFadden, L.A., Crockett, C.J., A'Hearn, M.F., Belton, M.J.S., Schultz, P., Lisse, C.M., 2007. Dust come morphology in the Deep Impact images of Comet 9P/Tempel 1. Icarus 187, 26–40.

Feaga, L.M., A'Hearn, M.F., Sunshine, J.M., Groussin, O., Farnham, T.L., 2007a. Asymmetries in the distribution of H_2O and CO_2 in the inner coma of Comet 9P/Tempel 1 as observed by Deep Impact. Icarus 190, 345–356.

Feaga, L.M., Groussin, O., Sunshine, J., A'Hearn, M.F., 2007b. Comparison of 9P/Tempel 1's IR spectra from Deep Impact synthetic models. Bull. Am. Astron. Soc. 39, 450.

Feldman, P.D., Lupu, R.E., McCandliss, S.R., Weaver, H.A., A'Hearn, M.F., Belton, M.J.S., Meech, K.J., 2006. Carbon monoxide in Comet 9P/Tempel 1 before and after the Deep Impact encounter. Astrophys. J. 647, 61–64.

Feldman, P.D., McCandliss, S.R., Route, M., Weaver, H.A., A'Hearn, M.F., Belton, M.J.S., Meech, K.J., 2007. Hubble Space Telescope observations of Comet 9P/Tempel 1 during the Deep Impact encounter. Icarus 187, 113–122.

Ghormley, J.A., 1968. Enthalpy changes and heat-capacity changes in the transformations from high-surface-area amorphous ice to stable hexagonal ice. J. Chem. Phys. 48, 503.

Gidaspow, D., 1994. Multiphase Flow and Fluidization. Academic Press, San Diego, CA.

Gougen, J.D., Thomas, P.C., Veverka, J.F., 2008. Flows on the nucleus of Comet Tempel 1. Lunar Planet. Sci. 39. Abstract #1969.

Gronkowski, P., 2005. The source of energy of the Comet 29P/Schwassmann–Wachmann 1 outburst activity: The test of the summary. Mon. Not. R. Astron. Soc. 360, 1153–1161.

Groussin, O., A'Hearn, M.F., Li, J.-Y., Thomas, P.C., Sunshine, J.M., Lisse, C.M., Meech, K.J., Farnham, T.L., Feaga, L.M., Delamere, W.A., 2007. Surface temperature of the nucleus of Comet 9P/Tempel 1. Icarus 187, 16–25.

Harker, D.E., Woodward, C.E., Wooden, D.H., 2005. The dust grains from 9P/Tempel 1 before and after the encounter with Deep Impact. Science 310, 278–280.

Iverson, R.M., LaHusen, R.G., 1989. Dynamic pore-pressure fluctuations in rapidly shearing granular materials. Science 246, 796–799.

Iverson, R.M., Reid, M.E., LaHusen, R.G., 1997. Debris-flow mobilization from landslides. Annu. Rev. Earth Planet. Sci. 25, 85–138.

Kearsley, A.T., Burchell, M.J., Hörz, F., Graham, G.A., Teslich, N., Cole, M.J., 2008. Stardust foil craters reveal the fine structure of dust from Comet Wild 2. In: Asteroids, Comets, Meteors (2008) Conference. Abstract #8158.

Keller, H.U., and 38 colleagues, 2007. Observations of Comet 9P/Tempel 1 around the Deep Impact event by the OSIRIS cameras onboard Rosetta. Icarus 187, 87–103.

Klinger, J., 1980. Some consequences of a phase transition of ice on the heat and mass balance of comets. Science 209, 271–272.

Kouchi, A., Greenberg, J.M., Yamamoto, T., Mukai, T., 1992. Extremely low thermal conductivity of amorphous ice: Relevance to comet evolution. Astrophys. J. 388, 73–76.

Lara, L.M., Boehnhardt, H., Gredel, R., Gutiérrez, P.J., Ortiz, J.L., Rodrigo, R., Vidal-Nuñez, M.J., 2006. Pre-impact monitoring of Comet 9P/Tempel 1, the Deep Impact target. Astron. Astrophys. 445, 1151–1157.

Laufer, D., Pat-El, I., Bar-Nun, A., 2005. Experimental simulation of the formation of non-circular active depressions on Comet Wild-2 and of ice grain ejection from cometary surfaces. Icarus 178, 248–252.

Lisse, C., 2002. On the role of dust mass loss in the evolution of comets and dusty disk systems. Earth Moon Planets 90, 497–506.

Lisse, C.M., A'Hearn, M.F., Groussin, O., Fernandez, Y.R., Belton, M.J.S., VanCleve, J.E., Charmandaris, V., Meech, K.J., McGleam, C., 2005. Rotationally resolved 8–35 micron Spitzer space telescope observations of the nucleus of Comet 9P/Tempel 1. Astrophys. J. 625, L139–L142.

McEwen, A.S., 1989. Mobility of large rock avalanches: Evidence from Valles Marineris, Mars. Geology 17, 1111–1114.

Meech, K.J., Wilson, L., Prialnik, D., 2008. Smooth regions on Comet 9P/Tempel 1: Cryovolcanic emplacement. In: Asteroids, Comets, Meteors (2008) Conference. Abstract #8341.

Melosh, H.J., 1986. The physics of very large landslides. Acta Mech. 64, 89–99.

Melosh, H.J., 1989. Impact Cratering: A Geologic Process. Oxford University Press, New York.

Mumma, M.J., and 13 colleagues, 2005. Parent volatiles in Comet 9P/Tempel 1: Before and after impact. Science 310, 270–274.

Patashnik, H., Rupprecht, G., Schuerman, D.W., 1974. Energy sources for comet outbursts. Nature 250, 313–314.

Prialnik, D., Bar-Nun, A., 1990. Gas release in comet nuclei. Astrophys. J. 363, 274–282.

Prialnik, D., Egozi, U., Bar-Nun, A., Podolak, M., Greenzweig, Y., 1993. On pore size and fracture in gas-laden cometary nuclei. Icarus 106, 499–507.

Prialnik, D., Benkhoff, J., Podolak, M., 2004. Modeling the structure and activity of comet nuclei. In: Festou, M.C., Keller, H.U., Weaver, H.A. (Eds.), Comets II. University of Arizona Press in collaboration with Lunar and Planetary Institute, Tucson and Houston, p. 359.

Richardson, J.E., Melosh, H.J., Lisse, C.M., Carcich, B., 2007. A ballistics analysis of the Deep Impact ejecta plume: Determining Comet Tempel 1's gravity, mass, and density. Icarus 190, 357–390.

Schleicher, D.L., Barnes, K.L., Baugh, N.F., 2006. Photometry and imaging results for Comet 9P/Tempel 1 and Deep Impact: Gas production rates, postimpact light curves, and ejecta plume morphology. Astron. J. 131, 1130–1137.

Schmitt, B., Espinasse, S., Grimm, R., Greenberg, J.M., Klinger, J., 1989. In: Hunt, J., Guyenne, T.D. (Eds.), Physics and Mechanics of Cometary Materials. ESA SP-302, p. 65.

Shreve, R.L., 1966. Sherman landslide, Alaska. Science 154, 1639–1643.

Sirono, S.-I., Greenberg, J.M., 2000. Do cometesimal collisions lead to bound rubble piles or to aggregates held together by gravity? Icarus 145, 230–238.

Sunshine, J.M., and 22 colleagues, 2006. Exposed water ice deposits on the surface of Comet 9P/Tempel 1. Science 311, 1453–1455.

Sunshine, J.M., Groussin, O., Schultz, P.H., A'Hearn, M.F., Feaga, L.M., Farnham, T.L., Klaasen, K.P., 2007. The distribution of water in the interior of Comet Tempel 1. Icarus 190, 284–294.

Tancredi, G., Rickman, H., Greenberg, J.M., 1994. Thermochemistry of cometary nuclei. I. The Jupiter family case. Astron. Astrophys. 286, 659–682.

Thomas, P.C., 1993. Gravity, tides, and topography on small satellites and asteroids: Application to surface features of the martian satellites. Icarus 105, 326–344.

Thomas, P.C., Veverka, J., Belton, M.J.S., Hidy, A., A'Hearn, M.F., Farnham, T.L., Groussin, O., Li, J.-Y., McFadden, L.A., Sunshine, J., Wellnitz, D., Lisse, C., Schlutz, P., Meech, K.J., Delamere, W.A., 2007. The shape, topography, and geology of Tempel 1 from Deep Impact observations. Icarus 187, 4–15.

Van der Bogert, C.H., Stephan, T., Jessberger, E.K., 2008. Capture-processing of Stardust cometary samples: Comparisons of capture-melted and unmelted particles. In: Asteroids, Comets, Meteors (2008) Conference. Abstract #8257.

Weissman, P.R., Asphaug, E., Lowry, S.C., 2004. Structure and density of cometary nuclei. In: Festou, M.C., Keller, H.U., Weaver, H.A. (Eds.), Comets II. University of Arizona Press in collaboration with Lunar and Planetary Institute, Tucson and Houston, p. 337.